lubricants

MDPI

Article

Effect of Electron Beam Irradiation on Friction and Wear Properties of Carbon Fiber-Reinforced PEEK at Different Injection Temperatures

Yi Chen [1,2,*,†], Jiahong Li [1,†], Da Bian [2,*] and Yongwu Zhao [2]

[1] School of Intelligent Manufacturing, Wuxi Vocational College of Science and Technology, Wuxi 214028, China
[2] School of Mechanical Engineering, Jiangnan University, Wuxi 214122, China
* Correspondence: chenyi_310@126.com (Y.C.); biand@jiangnan.edu.cn (D.B.)
† These authors contributed equally to this work.

Abstract

Polyetheretherketone (PEEK) is a high-performance engineering plastic widely used in aerospace, automotive, and other industries due to its heat resistance and mechanical strength. However, its high friction coefficient and low thermal conductivity limit its use in heavy-load environments. Existing studies have extensively explored the individual effects of thermal processing or irradiation on PEEK. However, the synergistic mechanism between the initial microstructure formed by mold temperature and subsequent irradiation modification remains unclear. This paper investigates the coupled effects of injection molding temperature and electron beam irradiation on the tribology of carbon fiber-reinforced PEEK composites, with the aim of identifying process conditions that improve friction and wear performance under high load by controlling the crystal morphology and cross-linking network. Carbon fiber (CF) particles were mixed with PEEK particles at a 1:2 mass ratio, and specimens were prepared at injection molding temperatures of 150 °C, 175 °C, and 200 °C. Some specimens were irradiated with an electron beam dose of 200 kGy. The friction coefficient, wear rate, surface shape, and crystallinity of the material were obtained using friction and wear tests, white-light topography, SEM, and XRD. The results show that the injection molding temperature of the material influences the friction performance. Optimal performance is obtained at 175 °C with a friction coefficient of 0.12 and wear rate of 9.722×10^{-6} mm^3/(N·m). After irradiation modification, the friction coefficient decreases to 0.10. This improvement is due to the moderate melt fluidity, adequate fiber infiltration, and dense crystallization at this temperature. In addition, cross-linking of chains occurs, and surface transfer films are created at this temperature. However, irradiation leads to a slight increase in wear rate to 1.013×10^{-5} mm^3/(N·m), suggesting that chain segment fracture and embrittlement effects are enhanced at this dose. At 150 °C, there is weak interfacial bonding and microcrack development. At 200 °C, excessive thermal motion reduces crystallinity and adds residual stress, increasing wear sensitivity. Overall, while irradiation reduces the friction coefficient, the wear rate is affected by the initial microstructure at molding. At non-optimal temperatures, embrittlement tends to dominate the wear mode. This study uncovers the synergistic and competitive dynamics between the injection molding process and irradiation modification, offering an operational framework and a mechanistic foundation for applying CF/PEEK under heavy-load conditions. The present approach can be extended in future work to other reinforcement systems or variable-dose irradiation schemes to further optimize overall tribological performance.

check for updates

Received: 11 November 2025
Revised: 11 December 2025
Accepted: 12 December 2025
Published: 16 December 2025

Citation: Chen, Y.; Li, J.; Bian, D.; Zhao, Y. Effect of Electron Beam Irradiation on Friction and Wear Properties of Carbon Fiber-Reinforced PEEK at Different Injection Temperatures. *Lubricants* **2025**, *13*, 546. https://doi.org/10.3390/lubricants13120546

Copyright: © 2025 by the authors. Licensee MDPI, Basel, Switzerland. This article is an open access article distributed under the terms and conditions of the Creative Commons Attribution (CC BY) license (https://creativecommons.org/licenses/by/4.0/).

Keywords: PEEK; CF; injection temperature; electron beam irradiation; friction coefficient; wear rate; transfer film; crystallinity

1. Introduction

PEEK is an aromatic hydrocarbon. Because of high aromatic rings in its main chain structure, the chemical stability of the PEEK structure is relatively high [1]. Due to its special molecular structure and crystallization properties, PEEK has good heat resistance, high strength, and wear resistance [2,3]. PEEK has high temperature resistance, corrosion resistance, and dimensional stability and thus is widely used in aerospace, automotive, medical, and other industries [4–6]. However, PEEK material still has some defects and shortcomings. For example, the friction coefficient of PEEK material is relatively high, and its thermal conductivity is poor [7]. When friction occurs, heat is generated and cannot dissipate quickly, which leads to failure and deformation of the PEEK material [8]. The PEEK material preparation process includes extrusion, injection molding, and compression molding [9]. With high-temperature forming processes such as injection molding, due to the large shrinkage rate, high melt viscosity, and poor fluidity of PEEK, it is difficult to achieve the desired microstructure and complete performance [10]. Therefore, expanding the application scope of PEEK is necessary. For example, when PEEK is used in heavy-load construction machinery, there are heavy demands on its mechanical strength and friction performance [11].

The present work on PEEK focuses on the modification of PEEK materials, and the optimization of production processes [12]. The inherent properties of the material have a significant influence on the performance of PEEK materials, and the product production process is related to performance [13]. The performance of PEEK composites is significantly affected by post-processing treatments and manufacturing parameters. Research indicates that heat treatment can greatly enhance the tribological properties of carbon fiber-reinforced PEEK (CF/PEEK). He et al. [14] discovered that annealing CF/PEEK composites improves wear resistance, which they attribute to increased crystallinity and hardness of the material. Additionally, the fabrication process is crucial for determining the final mechanical integrity. Lu et al. [15] investigated the mechanical properties of CF/PEEK composites prepared through hot-pressing pre-impregnated materials. They demonstrated that optimization of molding parameters, such as temperature and pressure, is essential for achieving superior performance by ensuring effective resin impregnation and minimizing voids. Yao et al. [16] explored how processing parameters impact the mechanical properties of CF/PEEK composites produced through hot compression molding. The investigation focused on different molding pressures and temperatures, revealing that these conditions significantly influence mechanical strength. The findings showed that inadequate molding pressure resulted in weak fiber–matrix interfacial bonding and a higher void content, which in turn reduced the composites' tensile and interlaminar shear strength. In recent years, irradiation techniques such as electron beam irradiation have been used for polymer modification. Such modification can induce cross-linking and crystallinity changes and improve the tribology [17–19].

Although the effects of processing temperature and irradiation on PEEK have been studied separately, the current literature rarely addresses the specific interaction between the in situ thermal history determined by injection mold temperature and subsequent irradiation modification. The injection mold temperature directly dictates the initial crystallinity, the skin–core structure, and the residual stress state of the molded part. These initial states crucially determine whether subsequent electron beam irradiation will predominantly

induce beneficial cross-linking or detrimental oxidative degradation. Incorporated properties of the material itself can have a significant influence on the performance of PEEK products. The production process of the product is also closely related to performance [20]. Therefore, stating the purpose of this study, investigating the injection molding processes of PEEK products and their interaction with irradiation treatment is of great importance for improving performance [21]. This study aims to bridge this gap by introducing a distinct approach that couples mold temperature regulation with irradiation. In this paper, CF/PEEK composite material splines were prepared under different injection molding temperatures. Electron beam radiation was applied and tensile tests on splines were performed with a universal testing machine. Surface tribological properties were studied for better performance. The interaction among material properties, injection molding temperature, and irradiation treatment was systematically analyzed to optimize the tribological performance of the composites [22–24].

2. Materials and Methods

2.1. Test Materials and Specimen Preparation

CF (T300; supplier: China Steel Group Engineering Technology Co., Ltd., Jilin, China) and PEEK powder (procured from Changchun Jida Special Plastics Engineering Research Co., Ltd., Changchun, China) were used. Injection molds were fabricated in accordance with ISO 527-2:2012 [25]. Surface-treated carbon fiber and PEEK powders were mixed at a mass ratio of 1:2 (CF:PEEK) until homogeneous. The blended mixture was then dried and fed into the injection molding machine. The mold temperature controller was set to mold temperatures of 150 °C, 175 °C, and 200 °C. These temperatures were selected based on the glass transition temperature (Tg) of PEEK to capture distinct crystallization behaviors: 150 °C represents a condition just below Tg in which crystallization kinetics are slow; 175 °C represents an optimal crystallization window; and 200 °C represents a high-temperature condition in which rapid spherulite growth or transcrystallization may occur, potentially inducing residual stresses. This range allows for the evaluation of the transition from amorphous-dominated to crystalline-dominated surface properties. A VI-55DRES injection molding machine (Zhongtai Precision Machinery [Guangzhou] Co., Ltd., Guangzhou, China) was used to prepare CF/PEEK composite test specimens. Subsequently, a portion of the molded strips was subjected to electron beam irradiation using an AB-5.0 accelerator (Wuxi Aibang Radiation Technology Co., Ltd., Wuxi, China; dose 200 kGy; energy 5 MeV). Both non-irradiated and irradiated specimens were obtained for testing.

2.2. Testing and Characterization

Friction and wear tests were carried out using an MFT-5000 multifunctional tribometer (MFT-5000, Rtec Instruments, San Jose, CA, USA) under dry sliding conditions. The test was performed in linear reciprocating mode with 9 mm diameter ceramic balls as the counterbody. The test parameters were as follows: normal load 50 N, frequency 2 Hz, duration 30 min, and stroke 5 mm. The MFP-D white-light profilometer was used to characterize the wear tracks and three-dimensional surface morphology and to determine the wear volume and the specific wear rate.

The wear rate (W) was calculated using the Archard wear equation (Equation (1)):

$$\mathrm{W} = \frac{V}{F \times S} = \frac{AL}{F \times S} \tag{1}$$

In the equation, W is the specific wear rate; V denotes the wear volume; S is the total sliding distance; F is the normal load, set to 50 N; the test was conducted at 2 Hz for

30 min. For the calculation of V, A denotes the cross-sectional area of the worn surface, obtained from three-dimensional profilometry; L denotes the effective track length used in the volume calculation, which in this reciprocating sliding test was taken as twice the stroke length. The cross-sectional profile of the worn surface was characterized using a three-dimensional profilometer and used to compute A. The schematic of the experimental principle is shown in Figure 1:

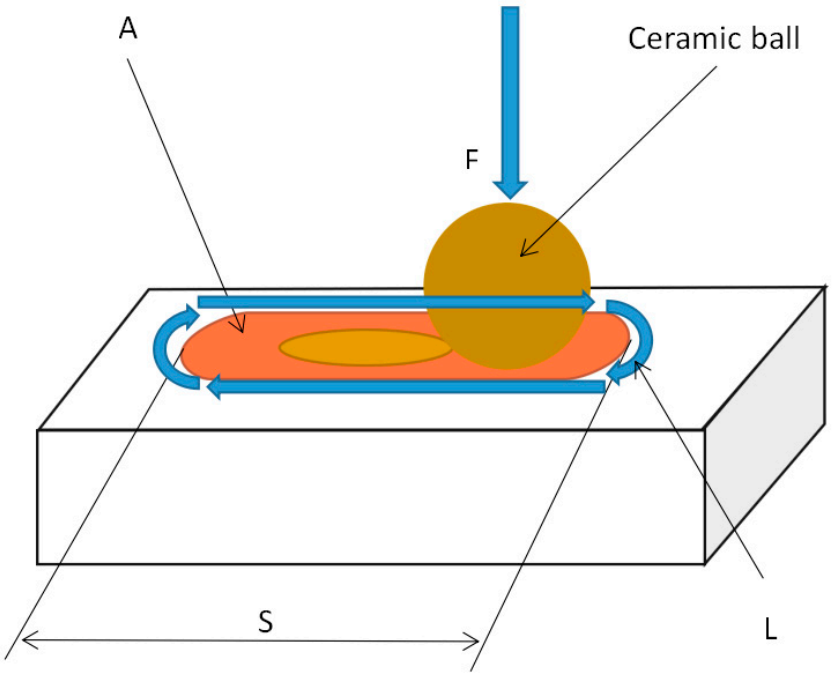


Figure 1. Schematic of the experimental principle.

Following the completion of the friction and wear test, the test specimen was examined with an MFP-D white-light profilometer (MFP-D, Rtec Instruments, San Jose, USA) to observe the wear track and three-dimensional topography of the composite material. The depth and width of the wear track were measured, and the wear rate was calculated from the profilometric data.

3. Analysis of Experimental Results

3.1. Analysis of the Friction Coefficient of PEEK Composites

Figure 2 shows the friction curves of PEEK composites processed at different injection molding temperatures, both before and after irradiation. Error bars representing the standard deviation of multiple measurements have been included to assess statistical significance. The data indicate that, for both pre- and post-irradiation samples, the steady-state friction coefficient first decreases and then increases with rising injection molding temperature. Prior to irradiation, at an injection molding temperature of 150 °C, the steady-state friction coefficient was approximately 0.39; at 175 °C, it was 0.12; and at 200 °C, it was 0.30. Post-irradiation, at an injection molding temperature of 150 °C, the friction coefficient was approximately 0.35; at 175 °C, it was 0.10; at 200 °C, the surface friction coefficient was 0.27. At a given injection molding temperature, the irradiated samples exhibited lower friction coefficients than their unirradiated counterparts. This is because irradiation-induced cross-linking and the formation of a transfer film predominantly reduce interfacial shear [26]; however, any adverse mechanical after-effects (such as embrittlement) are more pronounced in the wear rate rather than in the steady-state friction coefficient [27].

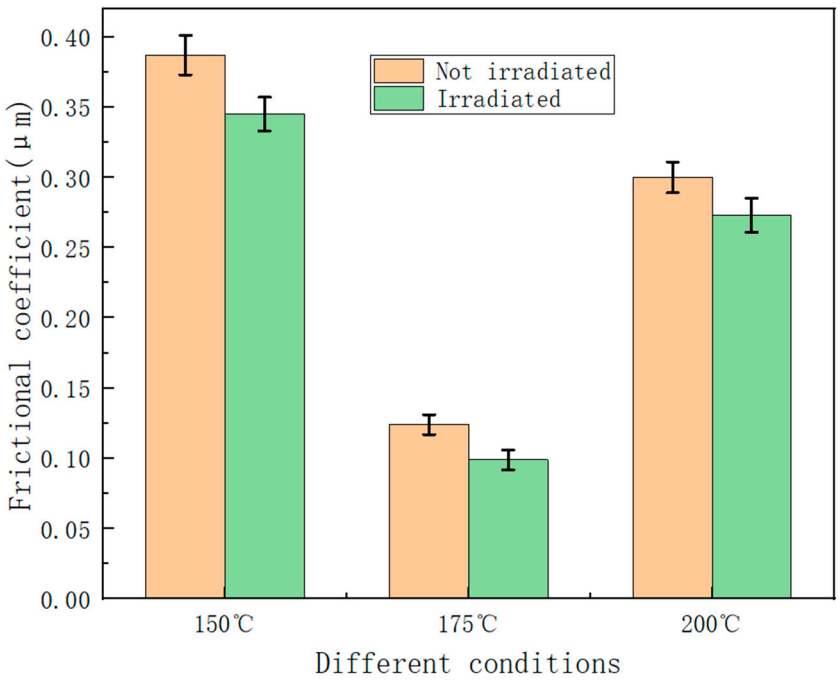
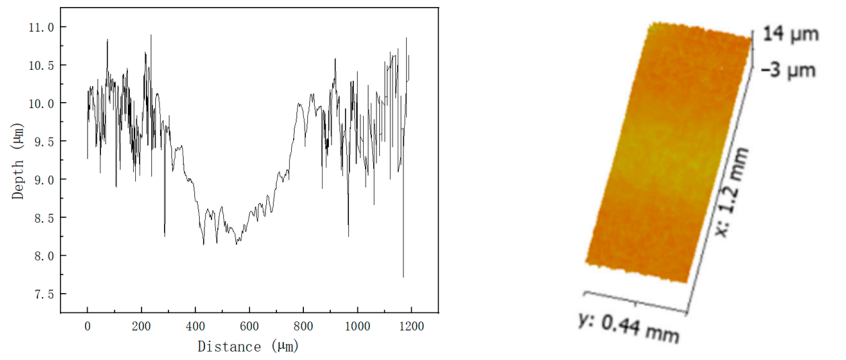


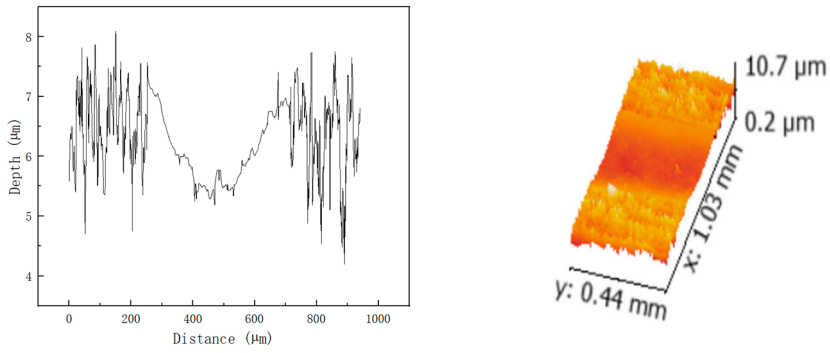
Figure 2. Comparison of friction coefficients of PEEK composites at different injection temperatures before and after irradiation.

3.2. Analysis of the Wear Resistance of PEEK Composites

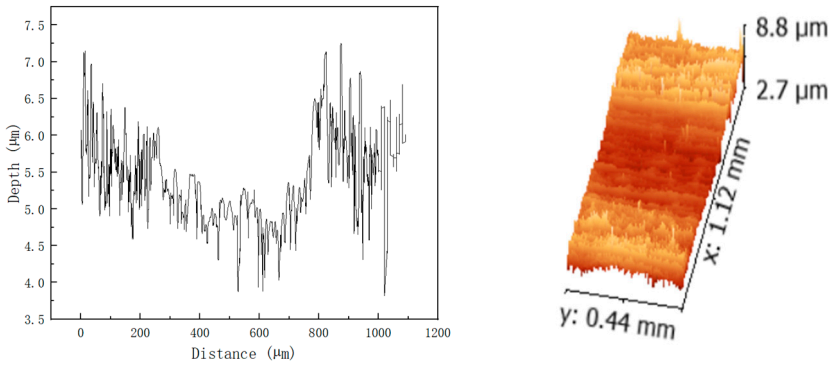
A material's wear resistance refers to its ability to resist material loss due to friction and is governed by the prevailing wear mechanisms [28]. A lower wear rate indicates superior wear resistance. This study evaluates the wear resistance of PEEK composite samples in terms of wear rate and wear volume. Figure 3 shows the wear track cross-sectional profiles and three-dimensional topography of PEEK composite samples produced at different injection molding temperatures before and after irradiation, under identical test conditions. The data reveal that, prior to irradiation, at an injection molding temperature of 150 °C, the post-test sample exhibited a wear track width of 900 μm and a depth of 2.2 μm, indicating a relatively wide track with pronounced grooves; at an injection molding temperature of 175 °C, the post-test wear track width was 700 μm, and the track depth was 2.5 μm, exhibiting a narrower track and less pronounced marks; at 200 °C, the post-test wear track width was 800 μm, and the track depth was 2.6 μm, with both track width and depth being relatively large and the grooves being pronounced. Post-irradiation, at an injection molding temperature of 150 °C, the wear track width of the tested sample was 700 μm, with a track depth of 2.6 μm. The track width was relatively large, and the marks were clearly visible. At an injection molding temperature of 175 °C, the post-test sample exhibited a wear track width of 760 μm and a track depth of 2.4 μm. The track width was reduced, and the depth was shallower. At an injection molding temperature of 200 °C, the post-test sample exhibited a wear track width of 840 μm and a depth of 2.5 μm, with both width and depth being substantial and the grooves being pronounced. Analysis of the wear-track cross-sectional profile data indicates that, in both the unirradiated and irradiated states, both width and depth first decrease and then subsequently increase with rising injection molding temperature.



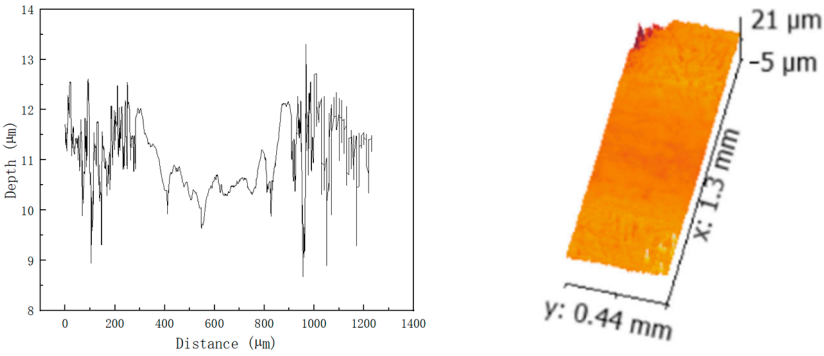
(**a**)



(**b**)



(**c**)



(**d**)

Figure 3. *Cont.*

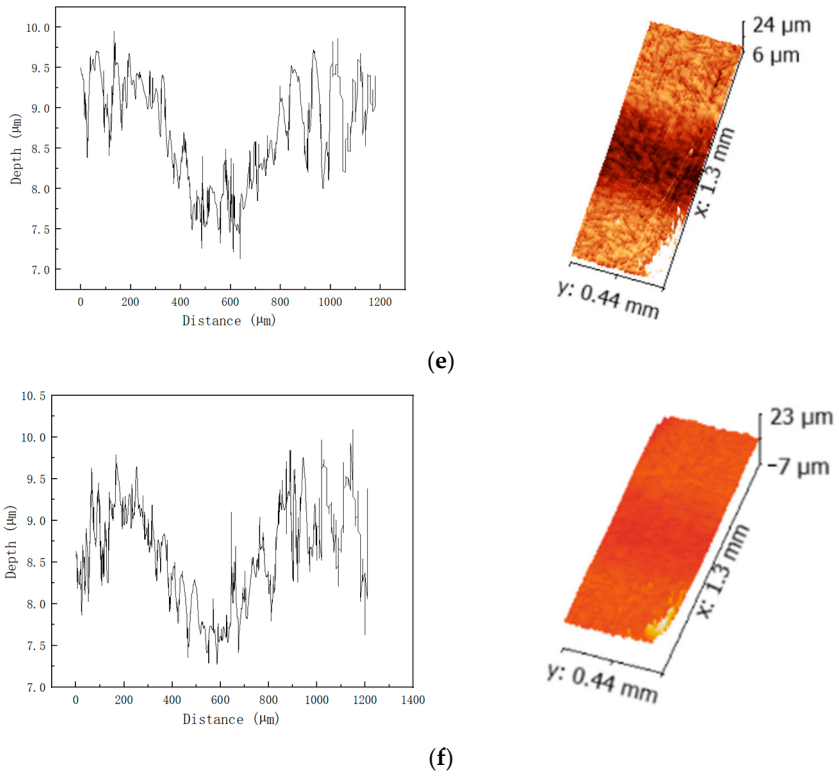


Figure 3. Comparison of cross-sections and 3D morphologies of wear marks before and after irradiation at different injection temperatures: (**a**) not irradiated at 150 °C; (**b**) irradiated at 150 °C; (**c**) not irradiated at 175 °C; (**d**) irradiated at 175 °C; (**e**) not irradiated at 200 °C; and (**f**) irradiated at 200 °C.

Based on the above data and Equation (1), the wear volume and wear rate of PEEK composite specimens molded at different injection molding temperatures were calculated as follows: Prior to irradiation, at an injection molding temperature of 150 °C, the wear rate was 1.100×10^{-11} $m^3/N.m$; at 175 °C, it was 9.722×10^{-6} $mm^3/(N \cdot m)$; at 200 °C, the wear rate was 1.156×10^{-5} $mm^3/(N \cdot m)$. Post-irradiation, at an injection molding temperature of 150 °C, the wear rate was 1.112×10^{-5} $mm^3/(N \cdot m)$; at 175 °C, it was 1.013×10^{-5} $mm^3/(N \cdot m)$; at 200 °C, it was 1.167×10^{-5} $mm^3/(N \cdot m)$. From 150 °C to 175 °C, the wear rate decreased with increasing temperature for both unirradiated and irradiated samples; from 175 °C to 200 °C, it increased with temperature.

Figure 4 shows the wear amount with error bars and Figure 5 illustrates the wear rates with error bars. Contrary to the significant reduction in friction coefficient, the changes in wear rate before and after irradiation are less distinct, with overlapping error bars in some conditions. For samples at the same injection molding temperature, the average wear rate prior to irradiation was slightly lower than or comparable to that after irradiation. As indicated by the slope of the trend lines in the figure, the temperature sensitivity of the average wear rate before irradiation is smaller than that after irradiation as the injection molding temperature varied [29]. Although only three temperature points were tested, these points effectively bracket the critical glass transition region and the optimal processing window, sufficiently capturing the non-linear "U-shaped" trend of the material's tribological behavior.

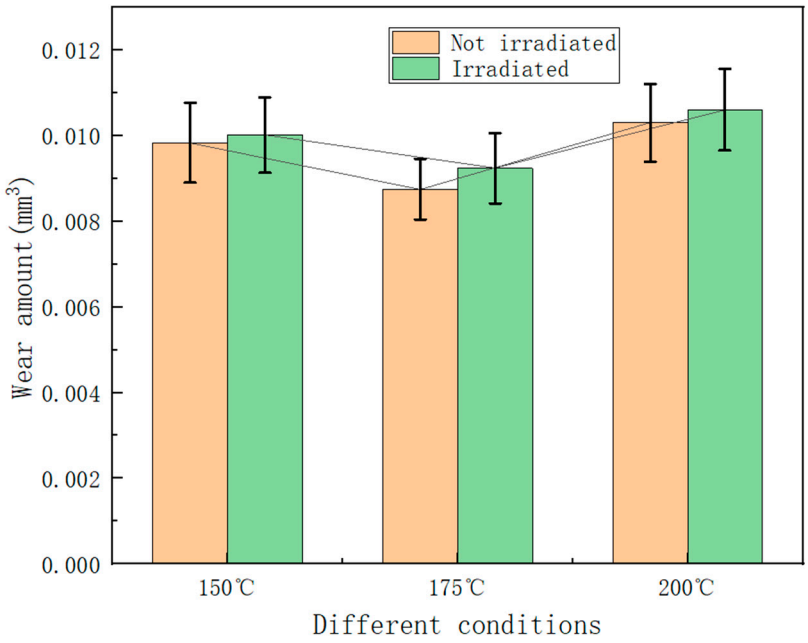


Figure 4. Comparison of wear amount before and after irradiation at different injection temperatures.

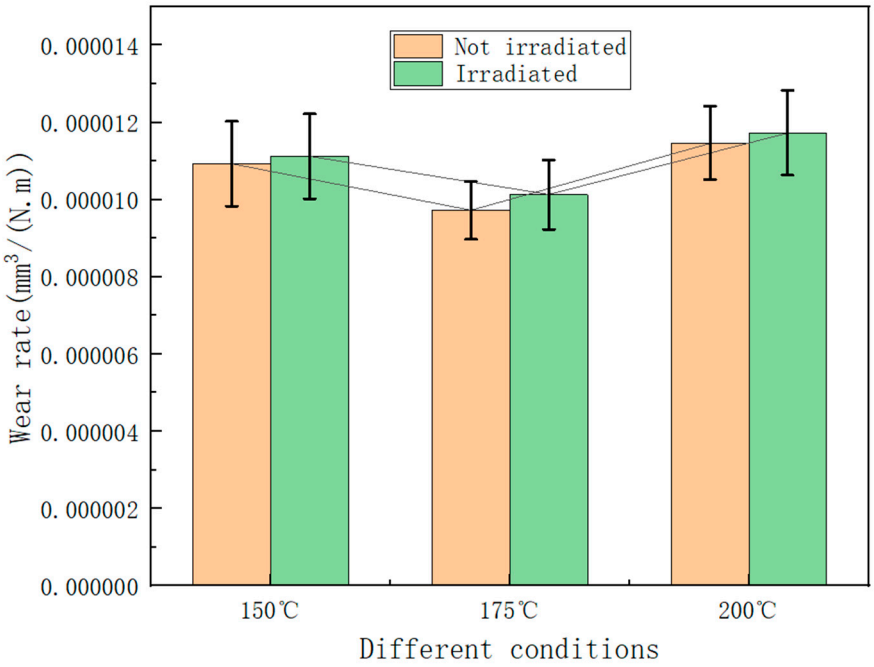


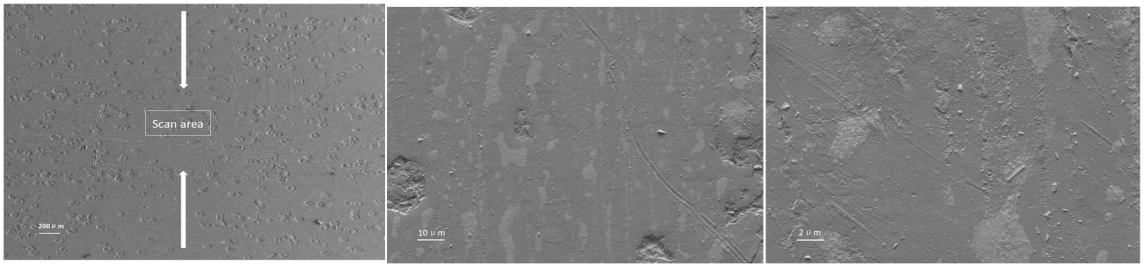
Figure 5. Comparison of wear rate before and after irradiation at different injection temperatures.

Figure 5 presents a comparison of wear rates for PEEK composite samples at different injection molding temperatures. This trend can be explained as follows: (1) Before and after irradiation, between 150 °C and 175 °C, increased molding temperatures enhance melt flowability while reducing adhesion. This elevates the crystallinity of the molded samples, resulting in higher strength and improved wear resistance and hence a lower wear rate with increasing injection molding temperature [30]. (2) For injection molding temperatures between 175 °C and 200 °C, both before and after irradiation, the process temperature surpasses PEEK's glass transition temperature. As the temperature rises, localized cross-linking and glass transition occur within the polymer matrix during cooling. Consequently, the mechanical properties deteriorate, reducing wear resistance. Thus, the wear rate increases with rising injection molding temperature [31]. (3) For samples at

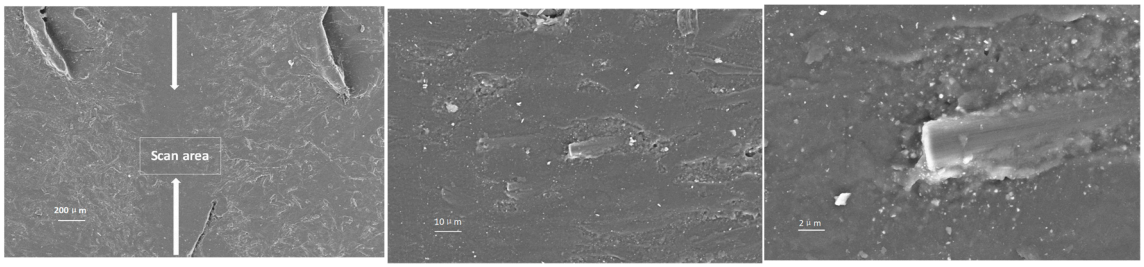
identical injection temperatures, the wear rate after irradiation is slightly higher than that before irradiation. This occurs because electron beam irradiation produces competing effects: while some cross-linking and the formation of a uniform, dense transfer film can reduce interfacial shear and lower the friction coefficient, chain scission and irradiation-induced embrittlement can dominate the wear response, promoting brittle fracture and fatigue crack propagation [32]. (4) The temperature sensitivity of the wear rate prior to irradiation is lower than that after irradiation as injection molding temperatures change. Excessive irradiation intensifies molecular chain scission, making the material brittle and reducing its toughness. As a result, wear primarily appears as brittle fracture and rapid fatigue crack propagation, causing a significant rise in the wear rate [33]. Nevertheless, the substantial overlap of error bars in Figures 4 and 5 indicates that the influence of irradiation on wear volume and specific wear rate is moderate rather than dramatic, and the conclusions regarding irradiation effects should therefore be regarded as trends rather than as statistically large differences.

3.3. SEM Analysis of Composite Worn Surfaces

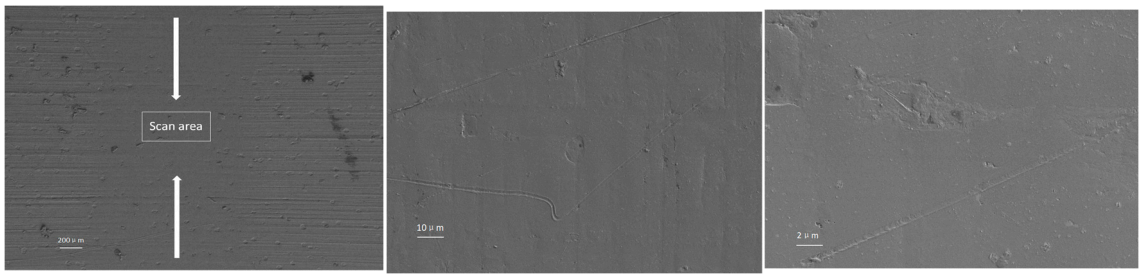
Figure 6 shows the SEM shape of surface wear marks on PEEK composite samples before and after electron beam irradiation. Figure 6a,c,e show the surface wear scar shape at injection molding temperatures of 150 °C, 175 °C, and 200 °C before and after irradiation. Figure 6b,d,f show the surface wear scar shape after irradiation. In all the images, the sliding direction is from up to down, and white arrows in the figure indicate the sliding direction.



(**a**)



(**b**)



(**c**)

Figure 6. *Cont.*

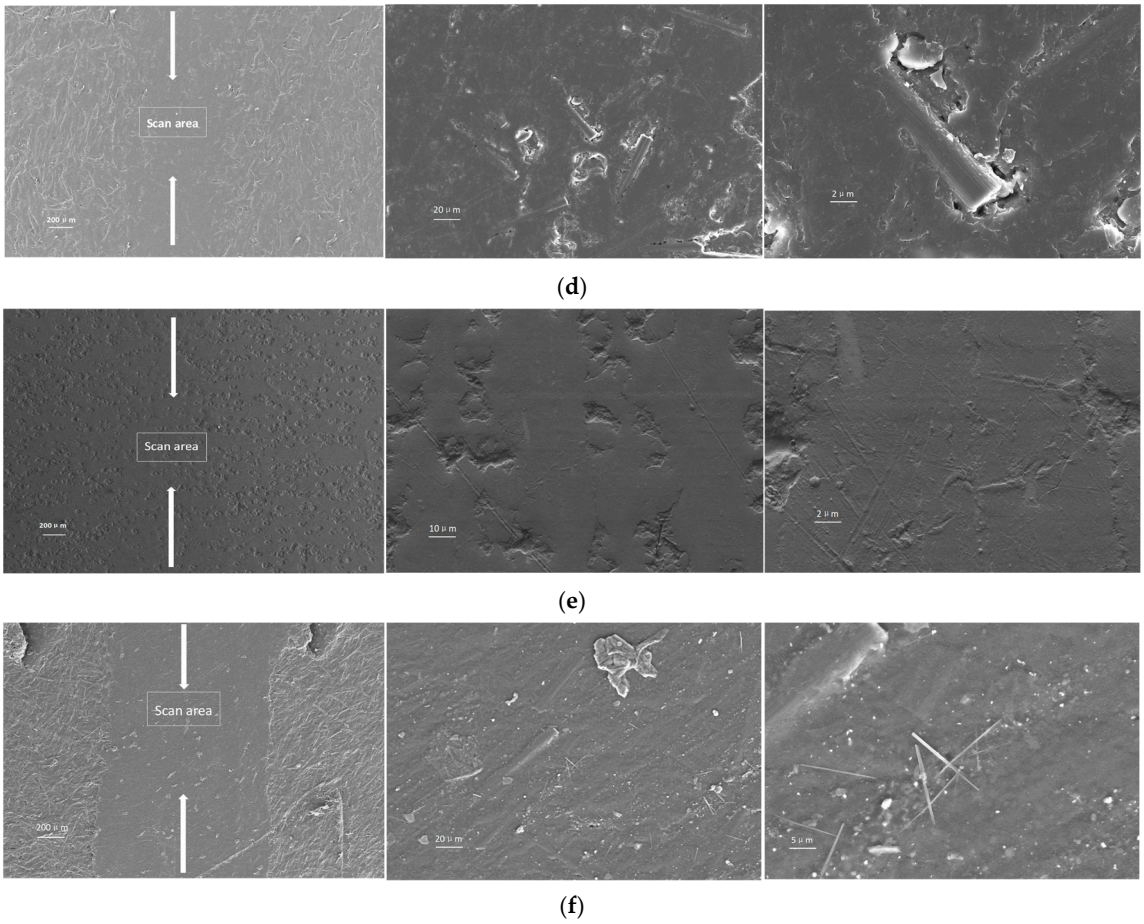


Figure 6. Comparison of SEM surface topography before and after irradiation at different injection temperatures: (**a**) not irradiated at 150 °C; (**b**) irradiated at 150 °C; (**c**) not irradiated at 175 °C; (**d**) irradiated at 175 °C; (**e**) not irradiated at 200 °C; and (**f**) irradiated at 200 °C.

At 150 °C, the unirradiated specimen (Figure 6a) exhibits a relatively wide and deep wear scar with pronounced furrow-like scratches and microcracks along the sliding direction. This morphology indicates severe material removal and a combination of abrasive and fatigue wear. The presence of exposed fibers and local delamination suggests poor interfacial bonding between the CF and the PEEK matrix, consistent with the low melt fluidity and insufficient impregnation at this molding temperature [34,35]. After irradiation (Figure 6b), the wear track still shows deep grooves and cracks, and the number of microcracks appears slightly increased. These features imply that electron beam irradiation introduces additional embrittlement into an already weak matrix, which promotes crack initiation and propagation under high contact stress [36,37].

At 175 °C, the unirradiated specimen (Figure 6c) displays a much smoother wear track compared with Figure 6a. The width and depth of the wear scar are smaller, and only minor cracks are visible. The worn surface exhibits areas of smeared material and relatively continuous transfer films, indicating a more stable sliding contact and improved load-bearing capacity. After irradiation (Figure 6d), the wear scar remains narrow and shallow, and the surface shows a more uniform transfer film with fewer large spalling pits. This suggests that the combination of optimal injection molding temperature and irradiation leads to a denser microstructure and a more coherent transfer film, thereby suppressing severe adhesive delamination and reducing friction [38]. At this temperature, higher crystallinity and stronger physical cross-linking enhance the mechanical strength,

so that a moderate irradiation dose predominantly improves surface hardness and transfer film stability rather than causing catastrophic embrittlement.

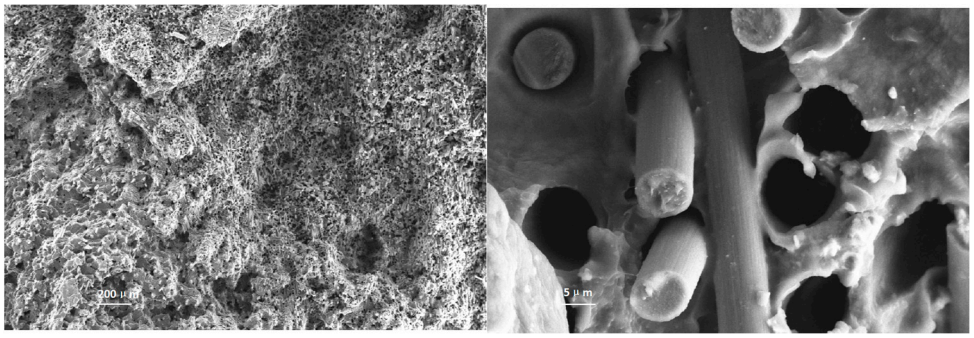
At 200 °C, the unirradiated specimen (Figure 6e) again exhibits a wider and deeper wear scar than at 175 °C, accompanied by pronounced grooves and local peeling. This morphology implies that an excessive molding temperature leads to the development of residual stresses and a less favorable crystalline structure, which decrease the material's resistance to repeated loading. After irradiation (Figure 6f), deeper peeling pits and more-fragmented surface features can be observed. This is attributed to the combined effects of thermal history and irradiation: when the injection molding temperature exceeds the glass transition temperature of PEEK, localized cross-linking and glass transition during cooling can induce internal stresses and structural heterogeneity, which are further aggravated by irradiation-induced chain scission, resulting in brittle fatigue wear [39].

Overall, the SEM observations confirm that the injection molding temperature plays a crucial role in determining melt flow, fiber wetting, crystallization behavior, and final microstructure and that electron beam irradiation superimposes additional cross-linking and chain scission effects on this initial microstructure. At the optimal temperature of 175 °C, irradiation improves surface integrity and promotes the formation of a stable transfer film, whereas at 150 °C and 200 °C, the dominant effect of irradiation is to enhance embrittlement and microcrack formation, slightly deteriorating wear resistance despite some reduction in the friction coefficient.

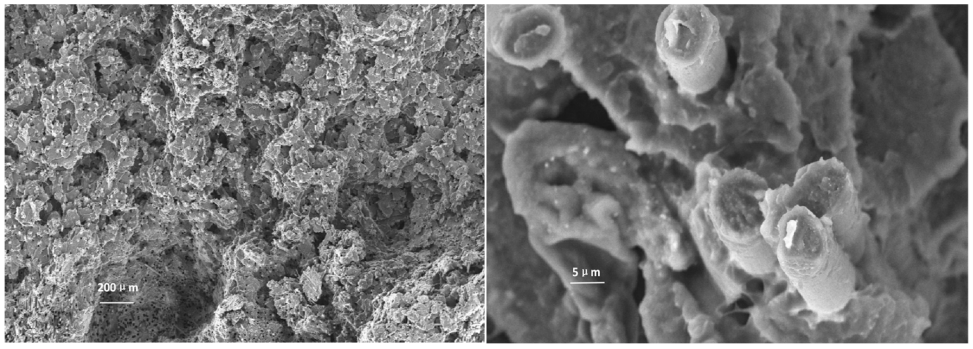
Figure 7 shows the SEM images of the cross-sectional morphology of PEEK composite splines at different injection molding temperatures before and after electron beam irradiation. In Figure 7a, obvious pores and exposed fibers can be seen in the cross-section; the CF distribution is uneven, and the interface bonding between the fibers and the resin matrix appears weak. Although it can be seen in Figure 7b that CF provides a certain skeletal support in the matrix, its wetting and coating effects are still not good, and there are still some areas with voids that have not been filled by resin. This is because, under the low-temperature injection molding conditions of 150 °C, the melt viscosity of PEEK is high and its fluidity is poor, making it difficult to fully penetrate and encapsulate the CF, resulting in insufficient interfacial bonding strength [40]. Under these conditions, the effect of electron beam irradiation on improving this inherent structural defect caused by insufficient fluidity is limited. The cross-sectional structure in Figure 7c is the densest, with almost no obvious pores observed. The CF is closely combined with the PEEK matrix, achieving excellent interfacial compatibility and stress transfer. In Figure 7d, as the content of functional components increases or their dispersion state changes, local agglomeration may occur, thereby introducing new micro-defects within the matrix. This is because, when the injection molding temperature is 175 °C, good fiber infiltration and matrix densification can be achieved. On this basis, moderate irradiation is expected to further consolidate this dense structure. However, if the additives are unevenly dispersed, irradiation may also fail to effectively eliminate the stress concentration points resulting from this [41]. In Figure 7e, the cross-section once again shows unevenness and a large number of pores. Figure 7f shows the presence of CF, but the completeness of the substrate coating seems to be in between that in other conditions. The higher injection molding temperature (200 °C) appears to induce additional voids and imperfect fiber wetting, likely due to excessive thermal motion and shrinkage during cooling. Electron beam irradiation at this stage can interact with the pre-existing defects and promote damage accumulation, leading to a less uniform cross-sectional morphology compared with that in the optimized 175 °C condition [41].

These SEM images show that the injection molding temperature plays an important role in melt flow, fiber wetting, crystallization behavior, and final microstructure. Electron beam irradiation, as a post-treatment modification, depends strongly on the initial

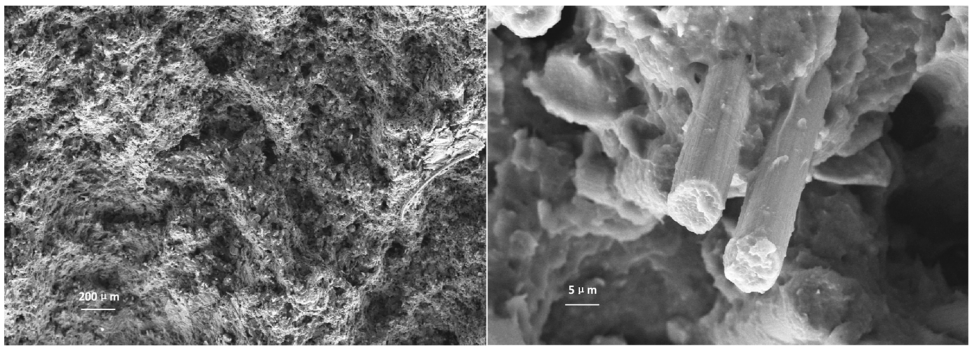
microstructure substrate formed during injection molding. At a suitable injection molding temperature (say 175 °C), the irradiation can play a positive role and further improve the tribological properties of the material [42].



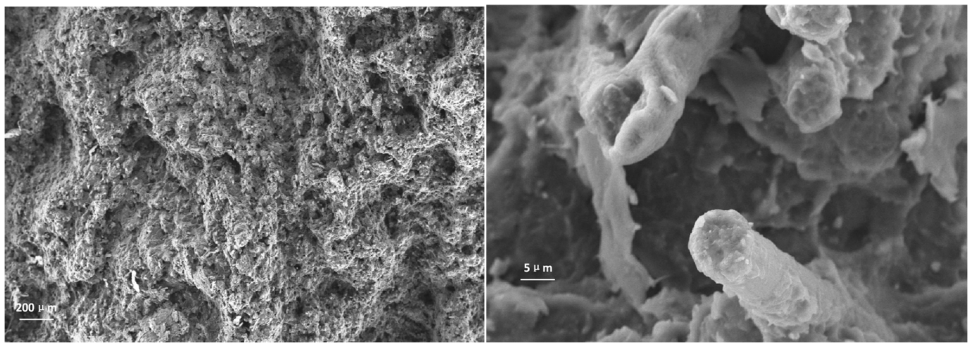
(**a**)



(**b**)



(**c**)



(**d**)

Figure 7. *Cont.*

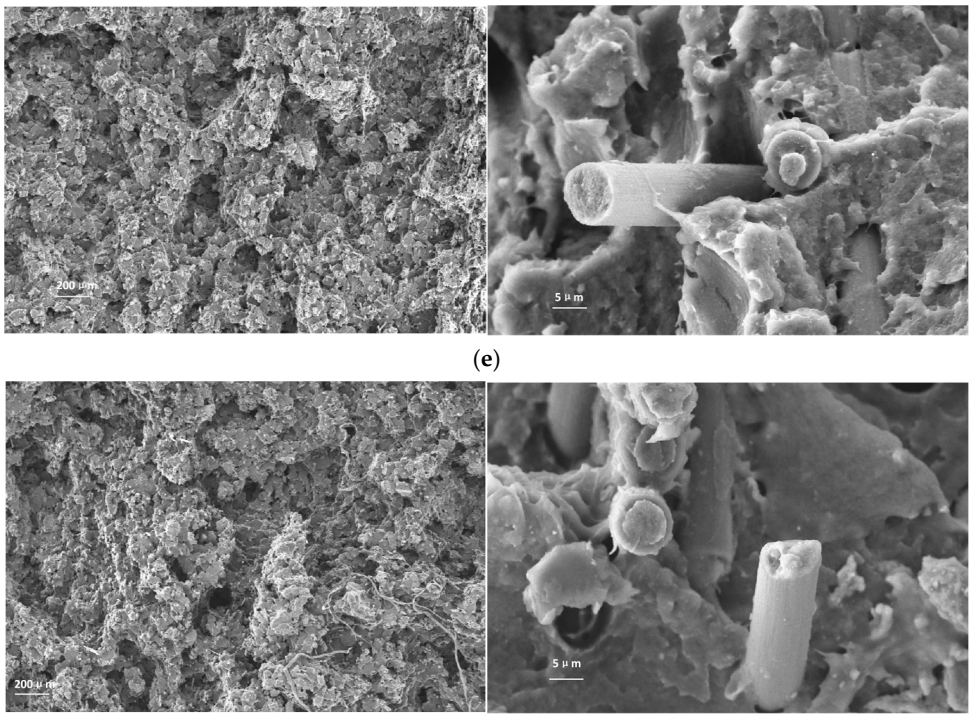


Figure 7. Cross-sectional SEM morphology comparison before and after electron beam irradiation at various injection temperatures: (**a**) not irradiated at 150 °C; (**b**) irradiated at 150 °C; (**c**) not irradiated at 175 °C; (**d**) irradiated at 175 °C; (**e**) not irradiated at 200 °C; and (**f**) irradiated at 200 °C.

Figure 8 shows XRD patterns of PEEK samples molded at different temperatures before and after electron beam irradiation. The characteristic diffraction peaks of PEEK occur at around 20° (2θ) in all samples, with additional weaker peaks possibly present at higher angles (e.g., 23°) depending on crystallite orientation. At the same molding temperature, irradiated samples exhibit significantly higher peak intensities than their unirradiated counterparts. For example, the peak intensity of the 150 °C-irradiated sample is nearly three times that of the unirradiated sample at the same temperature. Irradiated samples at 175 °C and 200 °C also show higher peak intensities than their unirradiated counterparts, though the difference is less pronounced than at 150 °C.

As the molding temperature increases from 150 °C to 200 °C, the intensity of these characteristic peaks gradually decreases for both unirradiated and irradiated samples, indicating very low crystallinity at higher temperatures (especially for 200 °C samples). The reason is that electron beam irradiation induces many free radicals on the PEEK molecular chain, which promote cross-linking and molecular rearrangement, increasing the number of crystallization centers and thus the crystallinity [43]. Higher molding temperatures cause excessive thermal motion in the PEEK molecular chain, disrupting the ordered crystallization structure and possibly inducing slight degradation, which inhibits crystallization. At 150 °C, irradiation effectively drives molecular chain rearrangement and enhances crystallinity. At 200 °C, however, irradiation may cause more-significant molecular chain degradation, which partially compensates for the crystallization enhancement induced by cross-linking [44].

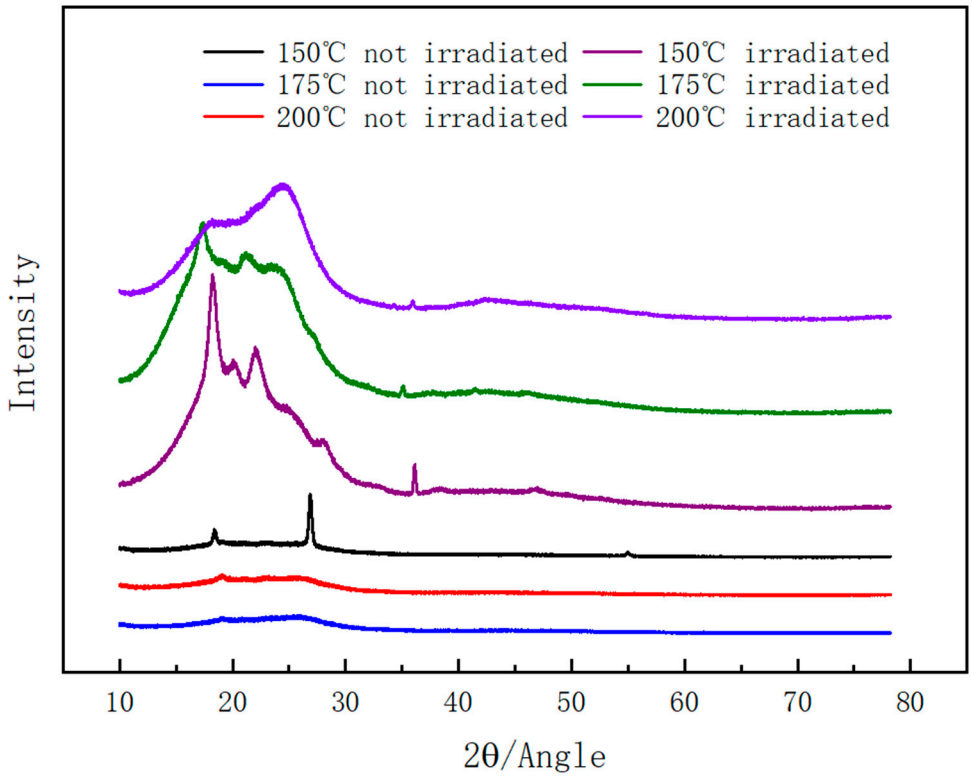


Figure 8. Comparison of XRD curves for different injection temperatures before and after electron beam irradiation.

4. Conclusions

The present study on CF-reinforced PEEK composites prepared under different injection molding temperatures and electron beam irradiation shows that both factors have a significant influence on the tribological properties of the composite. The experiments show that, at an injection molding temperature of 175 °C, the lowest friction coefficient (0.12 before irradiation and 0.10 after) and lowest specific wear rate (9.722×10^{-6} mm^3/(N·m) before irradiation and 1.013×10^{-5} mm^3/(N·m) after irradiation are obtained, showing superior wear resistance and surface integrity compared with those at 150 °C and 200 °C. This performance is due to the melt fluidity at this temperature, which allows uniform fiber wetting and dense crystallization. Electron beam irradiation induces molecular chain cross-linking, improves the hardness and lubrication of the transfer film, and optimizes the friction mechanism. Within the experimental scatter, irradiation produces a clear decrease in steady-state friction coefficient, while its effect on the specific wear rate is relatively modest. In some cases, the specific wear rate after irradiation is slightly higher than that before irradiation, which can be attributed to irradiation-induced chain scission and embrittlement that promote brittle fracture and fatigue wear. At 150 °C and 200 °C, the material properties suffer: low temperature fluidity leads to weak bonding, microcracks, and spalling, and high temperatures result in excessive thermal motion and residual stress that decrease crystallinity and increase wear sensitivity. Although irradiation lowers the friction coefficient, it may lead to brittleness or defects at non-optimal molding temperatures, thereby limiting its beneficial influence on wear resistance.

The results confirm the effect of injection molding process parameters and irradiation modification on the friction properties of PEEK and also provide guidance for engineering applications. For example, in aerospace or the heavy-duty machinery industry, an injection molding temperature of about 175 °C combined with appropriate irradiation can increase the durability of materials and reduce thermal failure risk. This work distinctively advances

the current understanding by providing a mechanistic framework that links the initial thermal processing history to the efficacy of subsequent irradiation modification, demonstrating that the optimal irradiation benefit is strictly dependent on the initial crystalline morphology. Future research could investigate different irradiation doses, alternative fiber or nanoparticle reinforcements, and a wider range of loads and sliding conditions to further clarify the relationship between microstructure and tribological behavior.

Limitations of this study should also be noted. First, only a single irradiation dose (200 kGy) and a limited range of molding temperatures (150–200 °C) were considered, so the conclusions are restricted to these processing windows. Second, all friction and wear tests were performed under one normal load and sliding speed without lubrication, and no detailed statistical hypothesis tests were conducted beyond the use of mean values and standard deviations. Finally, only SEM and XRD were used for microstructural characterization; additional techniques such as DSC or Raman spectroscopy could provide more quantitative information on crystallinity evolution. These limitations will be addressed in subsequent work.

Author Contributions: Conceptualization, Y.C. and D.B.; methodology, J.L. and Y.C.; software, Y.C.; validation, J.L. and D.B.; formal analysis, J.L. and D.B.; investigation, Y.C.; resources, J.L. and Y.Z.; data curation, J.L. and Y.C.; writing—original draft preparation, J.L. and Y.C.; writing—review and editing, J.L. and Y.C.; visualization, J.L. and Y.C.; supervision, Y.C.; project administration, Y.Z.; funding acquisition, D.B. and Y.Z. All authors have read and agreed to the published version of the manuscript.

Funding: Major projects of basic science research in colleges and universities of Jiangsu Province (24KJA460010), the National Natural Science Foundation of China (Grant No. 52205196), the Jiangsu Province Advanced Training Program for Professional Leaders Among Teachers in Higher Vocational Colleges (2024GRFX019), and the Jiangsu Province Blue and Green Project Outstanding Teaching Team (Su Jiao Shi Han [2024] No. 2).

Institutional Review Board Statement: Not applicable.

Informed Consent Statement: Not applicable.

Data Availability Statement: Data are contained within the article.

Conflicts of Interest: The authors declare no conflicts of interest.

References

1. Friedrich, K. Polymer composites for tribological applications. *Adv. Ind. Eng. Polym. Res.* **2018**, *1*, 3–39. [CrossRef]
2. Zhang, G.; Schlarb, A.K. Morphologies of the wear debris of polyetheretherketone produced under dry sliding conditions: Correlation with wear mechanisms. *Wear* **2009**, *266*, 745–752. [CrossRef]
3. Panin, S.V.; Nguyen, D.A.; Buslovich, D.G.; Alexenko, V.O.; Pervikov, A.V.; Kornienko, L.A.; Berto, F. Effect of Various Type of Nanoparticles on Mechanical and Tribological Properties of Wear-Resistant PEEK + PTFE-Based Composites. *Materials* **2021**, *14*, 1113. [CrossRef]
4. Kurtz, S.M. *PEEK Biomaterials Handbook*, 2nd ed.; William Andrew Publishing: Norwich, NY, USA, 2019.
5. Feng, C.; Guo, Y.; Yu, Z.; Chen, K.; Wang, D.; Li, X.; Luo, Y.; Wang, Q.; Zhang, D. Tribological properties of PEEK composites reinforced by MoS_2 modified carbon fiber and nano SiO_2. *Tribol. Int.* **2023**, *181*, 108315. [CrossRef]
6. Arif, M.F.; Alhashmi, H.; Varadarajan, K.M.; Koo, J.H.; Hart, A.J.; Kumar, S. Multifunctional performance of carbon nanotubes and graphene nanoplatelets reinforced PEEK composites enabled via FFF additive manufacturing. *Compos. Part B Eng.* **2020**, *184*, 107625. [CrossRef]
7. Lin, L.; Schlarb, A.K. The roles of rigid particles on the friction and wear behavior of short carbon fiber reinforced PBT hybrid materials in the absence of solid lubricants. *Tribol. Int.* **2018**, *119*, 404–410. [CrossRef]
8. Jiang, Z.; Jiang, B.; Yang, B.; Liu, X.; Yang, Y.; Zhang, C.; Shang, Y.; Zhang, H. Synergistically improving the thermal conductivity and mechanical strength of PEEK/MWCNT nanocomposites by functionalizing the matrix with fluorene groups. *Adv. Mater. Interfaces* **2023**, *10*, 2202508. [CrossRef]

9. Yang, J.; Xie, J.; Ji, K.; Wang, X.; Jiao, X.; Xu, Z.; Zhao, P. Microcellular injection molding of polyether-ether-ketone. *Polymer* **2022**, *251*, 124866. [CrossRef]
10. Guo, Z.; Xie, J.; Yang, J.; Fu, J.; Zhao, P. Rapid mold temperature rising method for PEEK microcellular injection molding based on induction heating. *J. Mater. Res. Technol.* **2023**, *26*, 3285–3300. [CrossRef]
11. Jin, Y.; Shen, W.; Yi, J.; Hou, Y.; Li, F. Significant tribological enhancement and mechanical property maintenance in polyether ether ketone (PEEK) matrix composites with minimal ultra-high-molecular-weight polyethylene (UHMWPE) incorporation. *Tribol. Trans.* **2024**, *67*, 1195–1207. [CrossRef]
12. Pajuste, E.; Reinholds, I.; Vaivars, G.; Antuzevičs, A.; Avotiņa, L.; Sprūģis, E.; Mikko, R.; Heikki, K.; Meri, R.M.; Kaparkalējs, R. Evaluation of radiation stability of electron beam irradiated Nafion® and sulfonated poly (ether ether ketone) membranes. *Polym. Degrad. Stab.* **2022**, *200*, 109970. [CrossRef]
13. Hu, J.; Zhang, H.; Li, S.; Ji, C.; Chen, S.; Zhou, Z.; Wang, B. Process parameter–mechanical property relationships and influence mechanism of advanced CFF/PEEK thermoplastic composites. *Polym. Compos.* **2022**, *43*, 5119–5132. [CrossRef]
14. He, Y.; Shen, M.; Wang, Q.; Wang, T.; Pei, X. Effects of FDM parameters and annealing on the mechanical and tribological properties of PEEK. *Compos. Struct.* **2023**, *313*, 116901. [CrossRef]
15. Lu, C.; Xu, N.; Zheng, T.; Zhang, X.; Lv, H.; Lu, X.; Xiao, L.; Zhang, D. The optimization of process parameters and characterization of high-performance CF/PEEK composites prepared by flexible CF/PEEK plain weave fabrics. *Polymers* **2018**, *11*, 53. [CrossRef]
16. Yao, S.S.; Jin, F.L.; Rhee, K.Y.; Hui, D.; Park, S.J. Recent advances in carbon-fiber-reinforced thermoplastic composites: A review. *Compos. Part B Eng.* **2018**, *142*, 241–250. [CrossRef]
17. Kurbanova, B.; Aimaganbetov, K.; Ospanov, K.; Abdrakhmanov, K.; Zhakiyev, N.; Rakhadilov, B.; Sagdoldina, Z.; Almas, N. Effects of electron beam irradiation on mechanical and tribological properties of PEEK. *Polymers* **2023**, *15*, 1340. [CrossRef]
18. Swan, S.R. Gamma Radiation Effects in Amorphous and Crystalline Polyaryletherketones. *Polym. Sci. Technol.* **2025**, *1*, 735–744. [CrossRef]
19. Chai, L.; Zhang, B.; Qiao, L.; Wang, P.; Weng, L. Influence of gamma irradiation-induced surface oxidation on tribological property of polyetheretherketone (PEEK). *Polym. Bull.* **2022**, *79*, 6513–6531. [CrossRef]
20. Shiv, J.K.; Kumar, K.; Jayapalan, S. Recent advances in tribological properties of silicon based nanofillers incorporated polymer nanocomposites. *Mater. Today Proc.* **2023**, *92*, 1231–1239. [CrossRef]
21. Rival, G.; Paulmier, T.; Dantras, E. Influence of electronic irradiations on the chemical and structural properties of PEEK for space applications. *Polym. Degrad. Stab.* **2019**, *168*, 108943. [CrossRef]
22. Sorayani Bafqi, M.S.; Birgun, N.; Saner Okan, B. Design and manufacturing of high-performance and high-temperature thermoplastic composite for aerospace applications. In *Handbook of Nanofillers*; Springer: Singapore, 2025; pp. 2931–2978.
23. Chai, L.; Ning, K.; Qiao, L.; Wang, P.; Weng, L. Comparative study on microstructure, mechanical, and tribological property of gamma-irradiated polytetrafluoroethylene, polyetheretherketone, and polyimide polymers. *Surf. Interface Anal.* **2022**, *54*, 13–24. [CrossRef]
24. Sathishkumar, S.; Jawahar, P.; Chakraborti, P. Influence of carbonaceous reinforcements on mechanical and tribological properties of PEEK composites–a review. *Polym.-Plast. Technol. Mater.* **2022**, *61*, 1367–1384. [CrossRef]
25. *ISO 527-2:2012*; Plastics—Determination of Tensile Properties—Part 2: Test Conditions for Moulding and Extrusion Plastics. International Organization for Standardization: Geneva, Switzerland, 2012.
26. Puhan, D.; Wong, J.S. Properties of Polyetheretherketone (PEEK) transferred materials in a PEEK-steel contact. *Tribol. Int.* **2019**, *135*, 189–199. [CrossRef]
27. Lv, M.; Zheng, F.; Wang, Q.; Wang, T.; Liang, Y. Effect of proton irradiation on the friction and wear properties of polyimide. *Wear* **2014**, *316*, 30–36. [CrossRef]
28. Chang, L.; Friedrich, K. Enhancement effect of nanoparticles on the sliding wear of short fiber-reinforced polymer composites: A critical discussion of wear mechanisms. *Tribol. Int.* **2010**, *43*, 2355–2364. [CrossRef]
29. Dai, J.N.; Kou, S.Q.; Yang, H.Y.; Xu, Z.B.; Shu, S.L.; Qiu, F.; Jiang, Q.C.; Zhang, L.C. High-content continuous carbon fibers reinforced PEEK matrix composite with ultra-high mechanical and wear performance at elevated temperature. *Compos. Struct.* **2022**, *295*, 115837. [CrossRef]
30. Li, M.; Zhang, K.; Ma, S.; Liu, G.; Yao, J.; Liu, H. Friction and wear behaviour of friction-induced crystallinity of polyaryl ether ketone (PAEK). *Wear* **2025**, 576–577, 206134. [CrossRef]
31. Jin, Z.; Yao, Z.; Sun, Y.; Shen, H. Loading capacity of PEEK blends in terms of wear rate and temperature. *Wear* **2022**, *496*, 204306. [CrossRef]
32. Almas, N.; Kurbanova, B.; Zhakiyev, N.; Rakhadilov, B.; Sagdoldina, Z.; Andybayeva, G.; Serik, N.; Alsar, Z.; Utegulov, Z.; Insepov, Z. Mechano-chemical properties of electron beam irradiated polyetheretherketone. *Polymers* **2022**, *14*, 3067. [CrossRef]
33. Lin, P.; Xu, Q.; Cheng, S.; Li, X.; Zhao, Z.; Sun, S.; Peng, C.; Joy, A.; Wang, S.Q. Effects of Molecular Weight Reduction on Brittle–Ductile Transition and Elastic Yielding Due to Noninvasive γ Irradiation on Polymer Glasses. *Macromolecules* **2017**, *50*, 2447–2455. [CrossRef]

34. Doumeng, M.; Ferry, F.; Delbé, K.; Mérian, T.; Chabert, F.; Berthet, F.; Marsan, O.; Nassiet, V.; Denape, J. Evolution of crystallinity of PEEK and glass-fibre reinforced PEEK under tribological conditions using Raman spectroscopy. *Wear* **2019**, *426*, 1040–1046. [CrossRef]
35. Sariyev, B.; Amrin, A.; Mergenbay, A.; Rao, H.J.; Khabdulayeva, A.; Spitas, C.; Golman, B. Thermal, hardness, and tribological assessment of PEEK/CoCr composites. *Sci. Rep.* **2025**, *15*, 28724. [CrossRef]
36. Lümkemann, N.; Eichberger, M.; Stawarczyk, B. Different PEEK qualities irradiated with light of different wavelengths: Impact on Martens hardness. *Dent. Mater.* **2017**, *33*, 968–975. [CrossRef]
37. Dong, W.; Nie, S.; Zhang, A. Tribological behavior of PEEK filled with CF/PTFE/graphite sliding against stainless steel surface under water lubrication. *Proc. Inst. Mech. Eng. Part J J. Eng. Tribol.* **2013**, *227*, 1129–1137. [CrossRef]
38. Qu, S.; Lo, K.H.; Wang, S.S. Effect of transfer films on friction of PTFE/PEEK composite. *J. Tribol.* **2021**, *143*, 041401. [CrossRef]
39. Chen, Y.K.; Lin, G.B.; Shukur, Z.M.; Kukureka, S.N.; Dearn, K.D. Wear and Friction Behaviour of Additive Manufactured PEEK under Non-conformal Contact. *J. Phys. Conf. Ser.* **2024**, *2692*, 012046. [CrossRef]
40. Zarges, J.C.; Sälzer, P.; Heim, H.P. Correlation of fiber orientation and fiber-matrix-interaction of injection-molded polypropylene cellulose fiber composites. *Compos. Part A Appl. Sci. Manuf.* **2020**, *139*, 106112. [CrossRef]
41. Wang, Z.; Muránsky, O.; Zhu, H.; Wei, T.; Zhang, Z.; Ionescu, M.; Yang, C.; Davis, J.; Hu, G.; Munroe, P.; et al. Impact of pre-existing crystal lattice defects on the accumulation of irradiation-induced damage in a C/C composite. *J. Nucl. Mater.* **2022**, *564*, 153684. [CrossRef]
42. Guo, M.; Yang, L.; Yang, Z.; Zhang, D.; Wang, Q.; Li, P.; Zhao, P.; Yang, M.; Li, Y. Tribological behaviors of oxygen-doped carbon coatings deposited by ion-irradiation-assisted growth. *Surf. Coat. Technol.* **2021**, *425*, 127689. [CrossRef]
43. Rakhadilov, B.; Ormanbekov, K.; Zhassulan, A.; Andybayeva, G.; Shynarbek, A.; Mukhametov, Y.M.Y. Influence of irradiation doses on the mechanical and tribological properties of polyetheretherketone exposed to electron beam treatment. *Adv. Sci. Technol. Res. J.* **2025**, *19*, 121–131. [CrossRef] [PubMed]
44. Vieille, B.; Coppalle, A. Influence of temperature degradation on the low velocity impact behavior of hybrid thermoplastic PEEK laminates. *J. Thermoplast. Compos. Mater.* **2024**, *37*, 146–166. [CrossRef]

Disclaimer/Publisher's Note: The statements, opinions and data contained in all publications are solely those of the individual author(s) and contributor(s) and not of MDPI and/or the editor(s). MDPI and/or the editor(s) disclaim responsibility for any injury to people or property resulting from any ideas, methods, instructions or products referred to in the content.